Electronic structure of monolayer and bilayer graphene on hexagonal substrates

Marcin Mucha-Kruczynski

UNIVERSITY OF BATH

J.R. Wallbank, A.A. Patel, A.K. Geim, V.I. Fal'ko

J.R. Wallbank et al., PRB 87, 245408 (2013)
MM-K et al., arXiv:1304.1734

Motivation

hBN as a substrate for graphene:

- C.R. Dean et al., Nature Nanotech. **5**, 722 (2010),
- A.S. Mayorov et al., Nano Letters **11**, 2396 (2011),

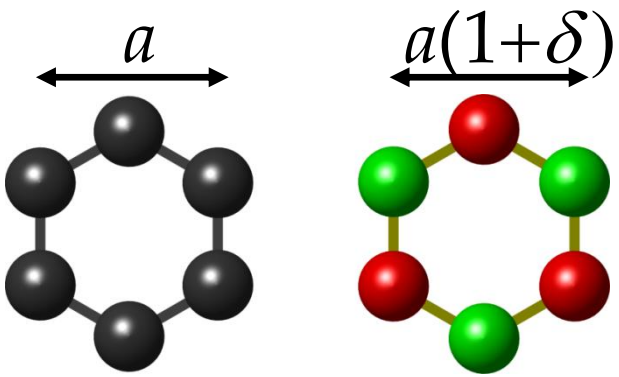

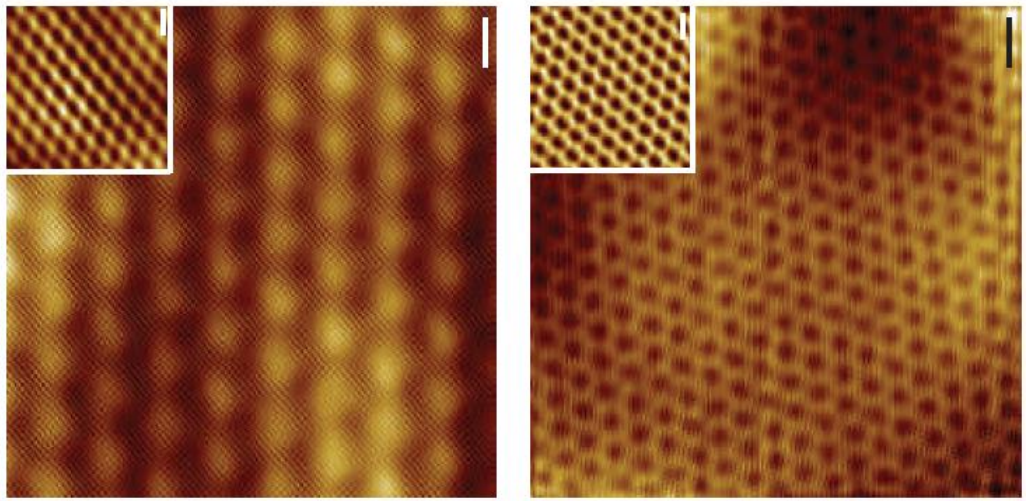

J. Xue et al., Nature Mater. **10**, 282 (2011)

MLG/hBN

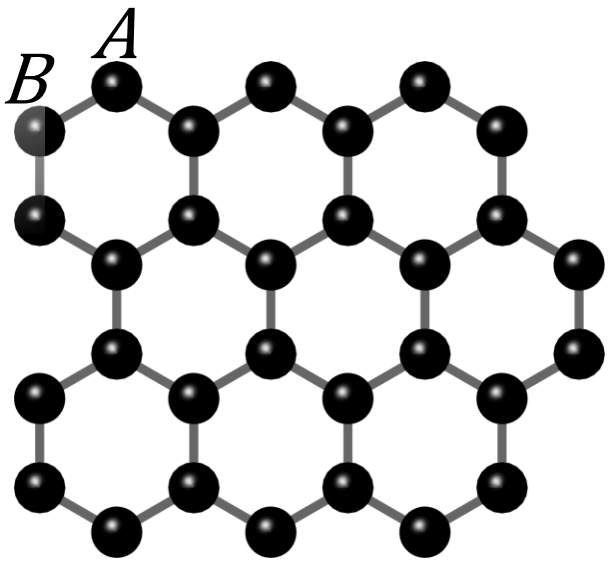

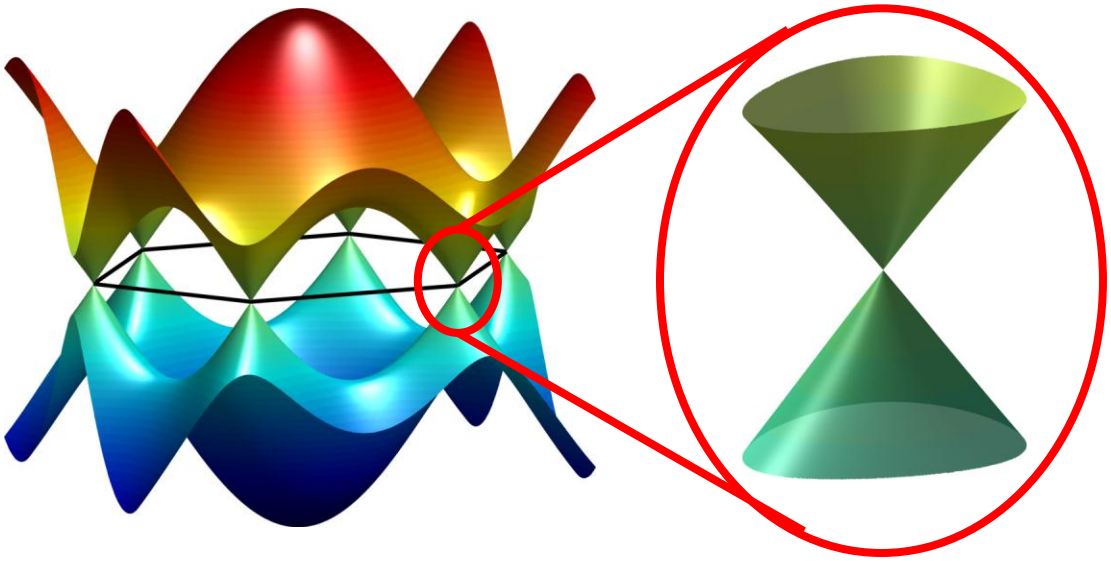

$$\hat{\boldsymbol{H}}_{\mathrm{MLG}} = v \begin{pmatrix} 0 & p_x - ip_y & 0 & 0 \\ p_x + ip_y & 0 & 0 & 0 \\ 0 & 0 & 0 & p_x - ip_y \\ 0 & 0 & p_x + ip_y & 0 \end{pmatrix} = v\boldsymbol{\sigma}\cdot\boldsymbol{p} \otimes \mathbb{1}$$

Model of the moiré perturbation

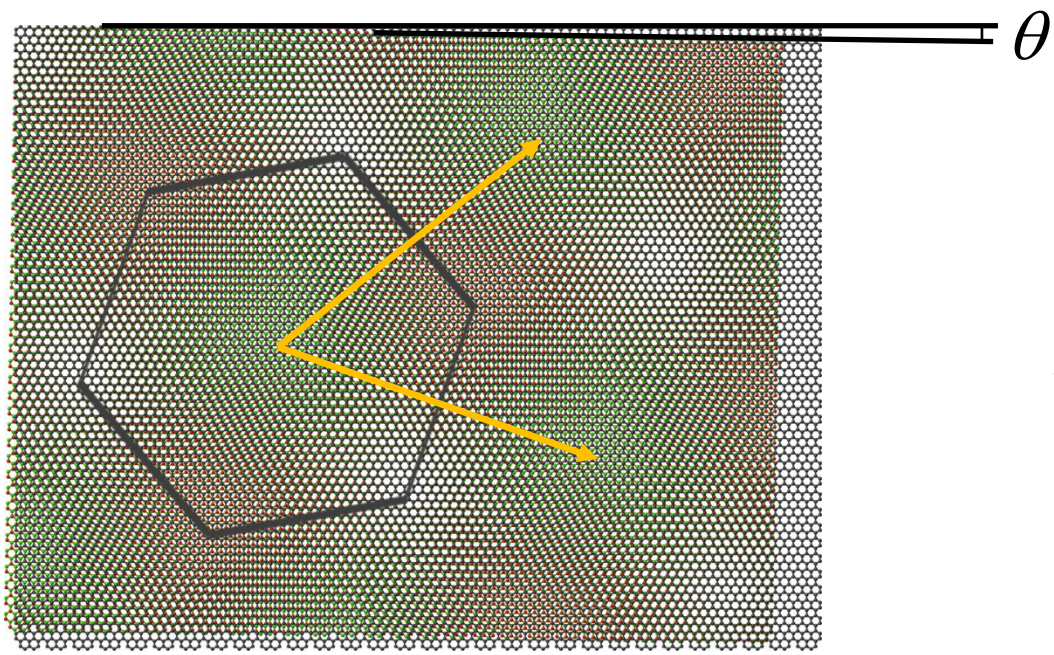

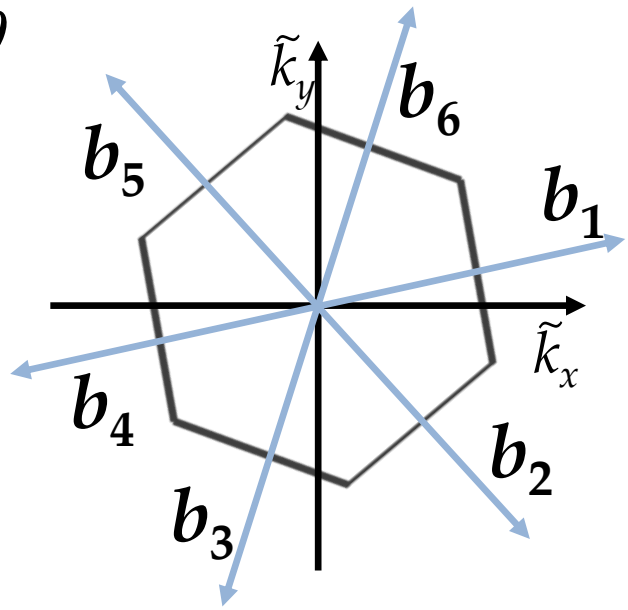

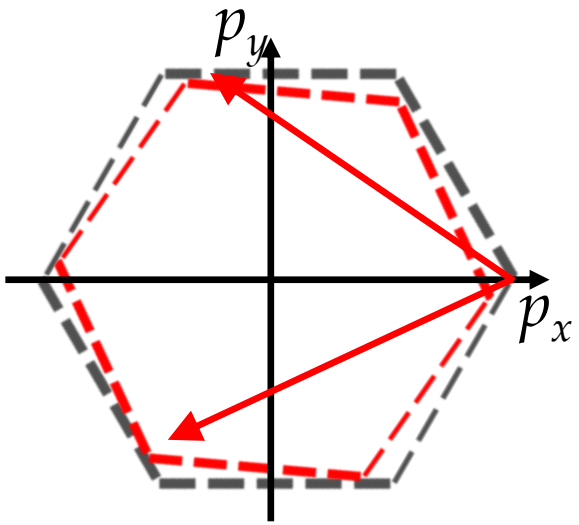

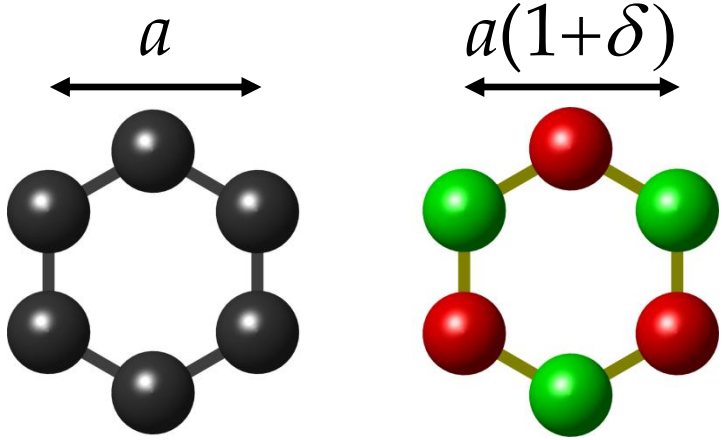

Model of the moiré perturbation

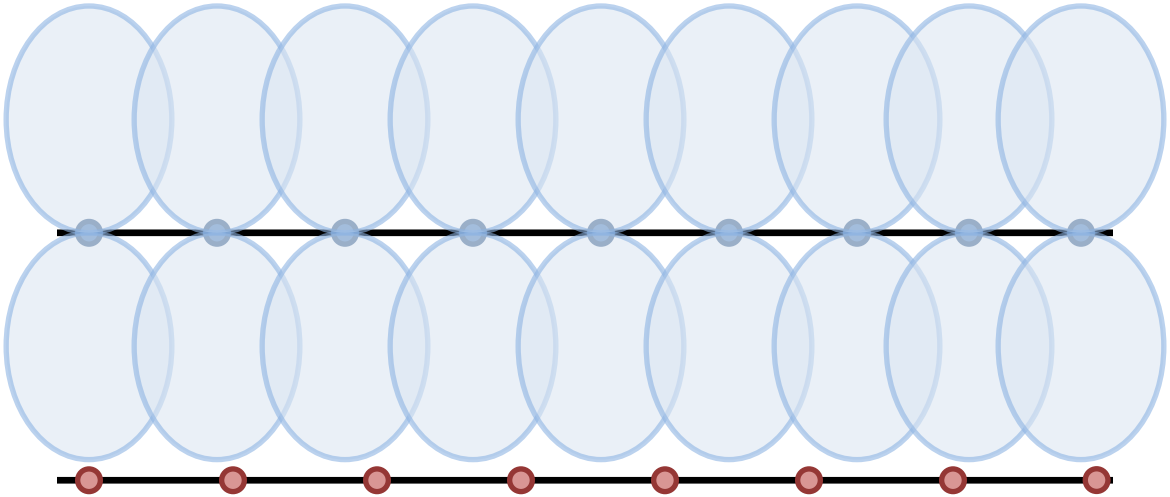

1. Potential felt by electrons is smooth on the scale of moiré
2. The first harmonic of the moiré dominant, no intervalley terms

Twisted BLG: J.M.B. Lopes dos Santos et al., PRL **99**, 256802 (2007),
R. Bistritzer and A.H. MacDonald, PRB **81**, 245412 (2010),
P. Moon and M. Koshino, PRB **85**, 195458 (2012)

MLG/hBN: C. Ortix et al., PRB **86**, 081405 (2012),
M. Kindermann et al., PRB **86**, 115415 (2012),
M. Yankowitz et al., Nature Phys. **8**, 382 (2012),

Model of the moiré perturbation

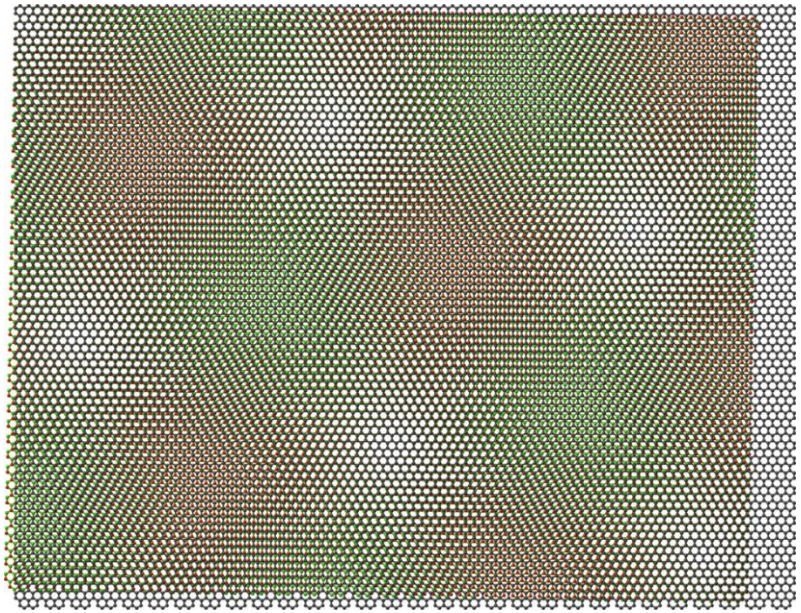

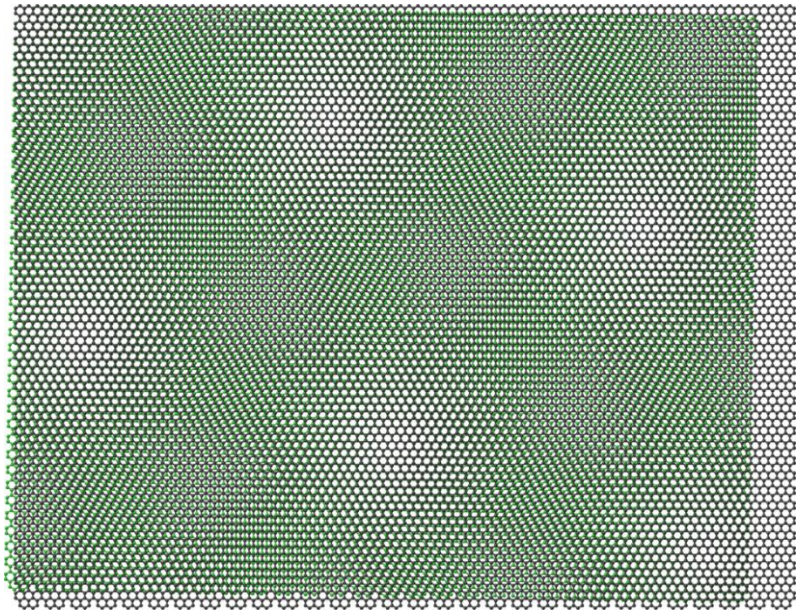

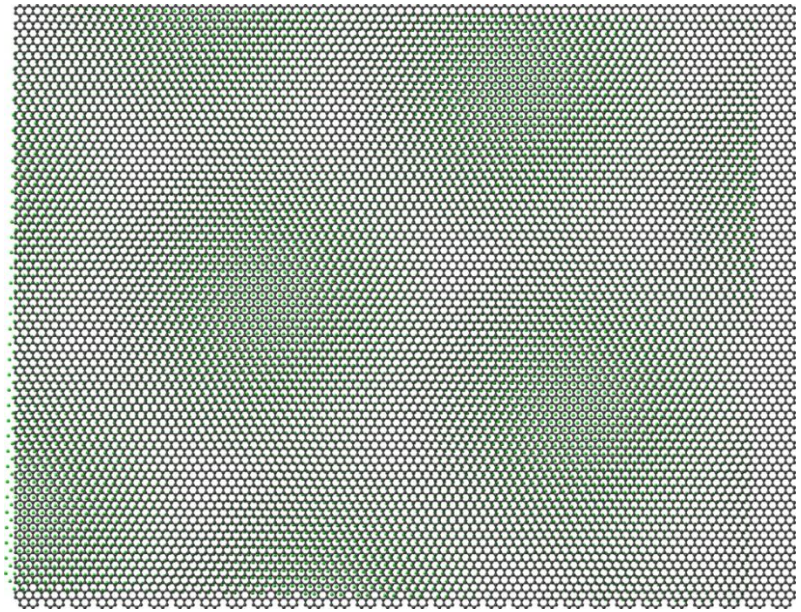

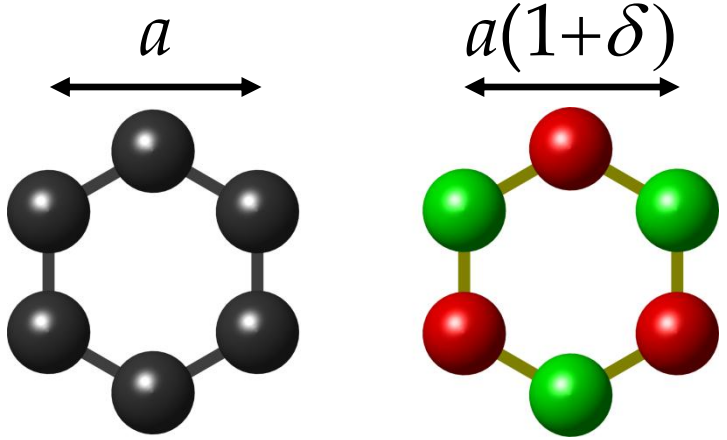

MLG/hBN

$$\hat{H} = v\boldsymbol{p}\cdot\boldsymbol{\sigma} + u_0 v b f_1(\boldsymbol{r}) + u_3 v b f_2(\boldsymbol{r})\sigma_3\tau_3 + u_1 v\left[\boldsymbol{l}_z \times \nabla f_2(\boldsymbol{r})\right]\cdot\boldsymbol{\sigma}\tau_3$$

Dirac part

Magnitude of potential

Local sublattice asymmetry

Hopping modulation

$$f_1(\boldsymbol{r}) = \sum_{n=1}^{6} e^{i\boldsymbol{b_n}\cdot\boldsymbol{r}}, \qquad f_2(\boldsymbol{r}) = i\sum_{n=1}^{6}(-1)^n e^{i\boldsymbol{b_n}\cdot\boldsymbol{r}},$$

$$vb \approx 2\pi\sqrt{\delta^2+\theta^2}\gamma_0$$

$$\epsilon_{\boldsymbol{K}+\boldsymbol{p}}^{u_0,u_1,u_3} = -\epsilon_{\boldsymbol{K}-\boldsymbol{p}}^{-u_0,-u_1,u_3} = -\epsilon_{\boldsymbol{K}+\boldsymbol{p}}^{-u_0,u_1,-u_3} = \epsilon_{\boldsymbol{K}-\boldsymbol{p}}^{u_0,-u_1,-u_3}$$

J.R. Wallbank et al., PRB **87**, 245408 (2013)

MLG/hBN

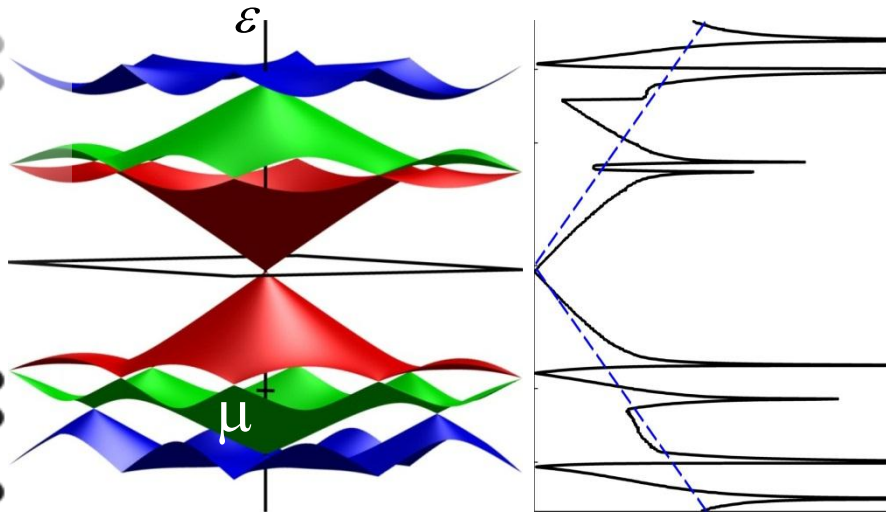

DoS

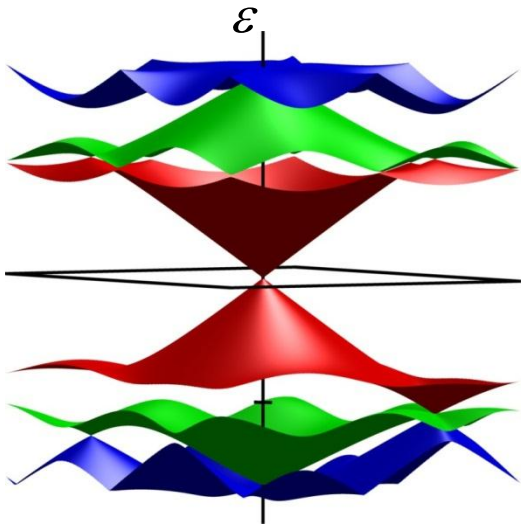

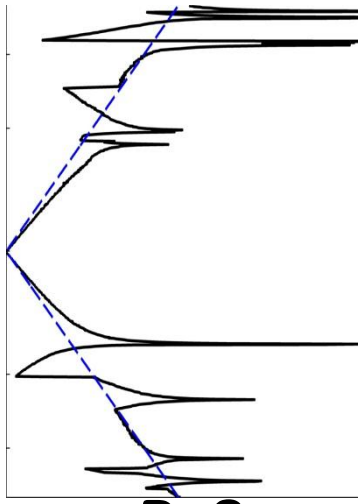

DoS

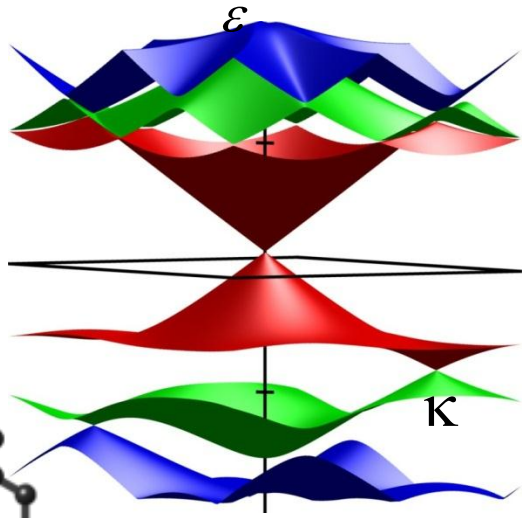

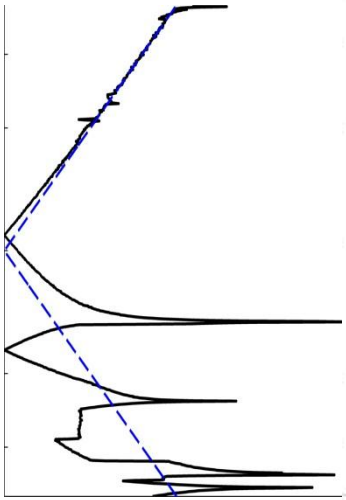

DoS

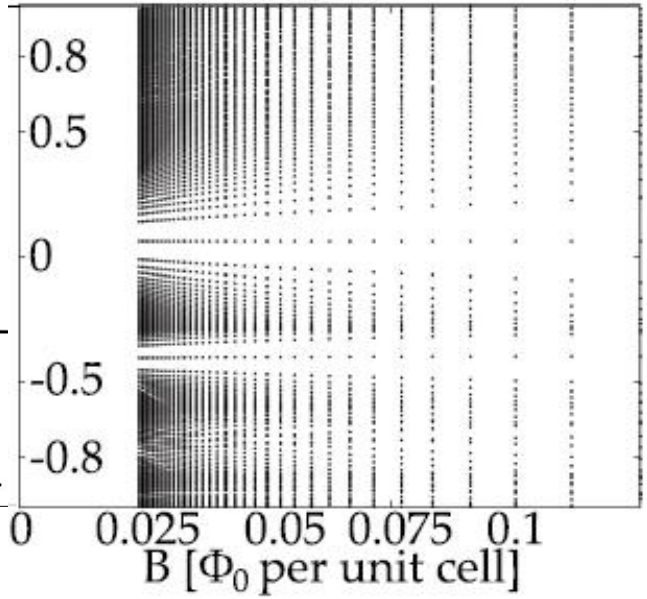

MLG/hBN

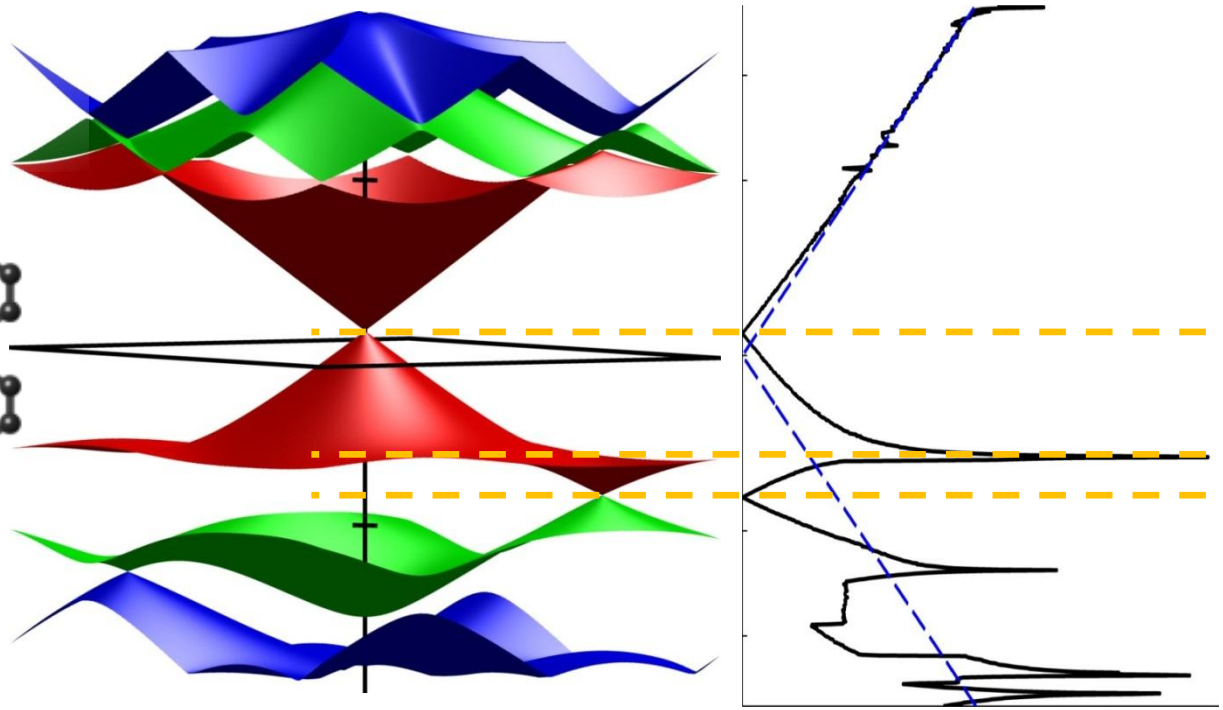

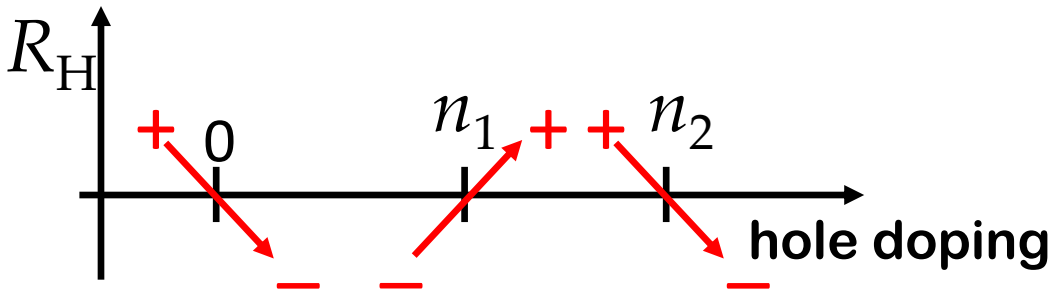

MLG/hBN

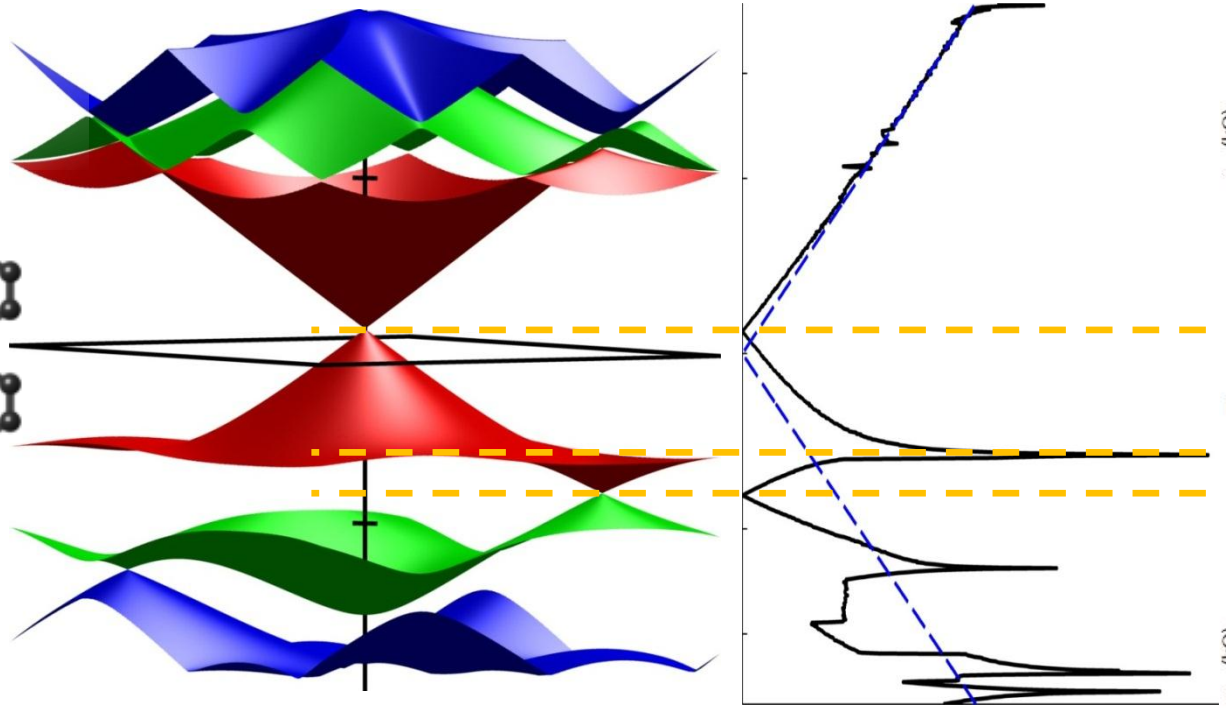

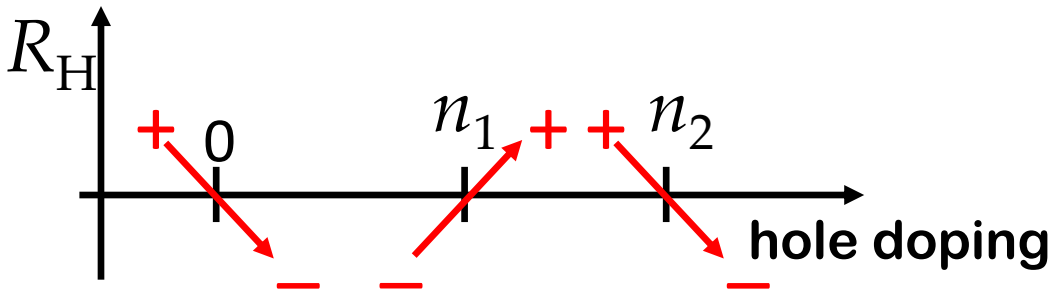

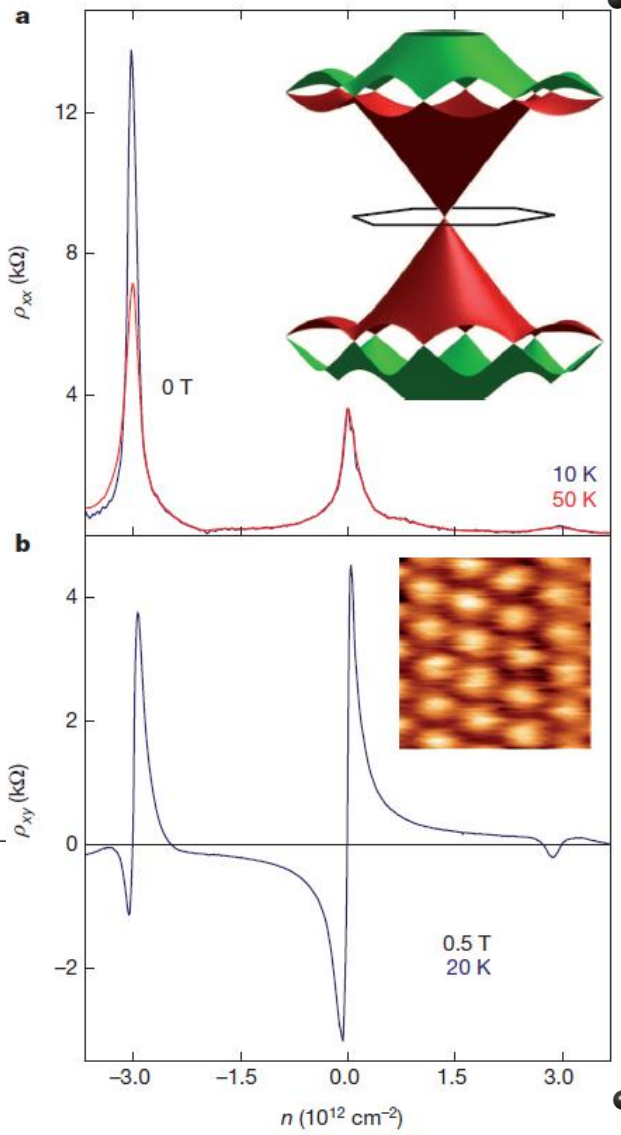

L.A. Ponomarenko et al., Nature **497**, 594 (2013)

MLG/hBN

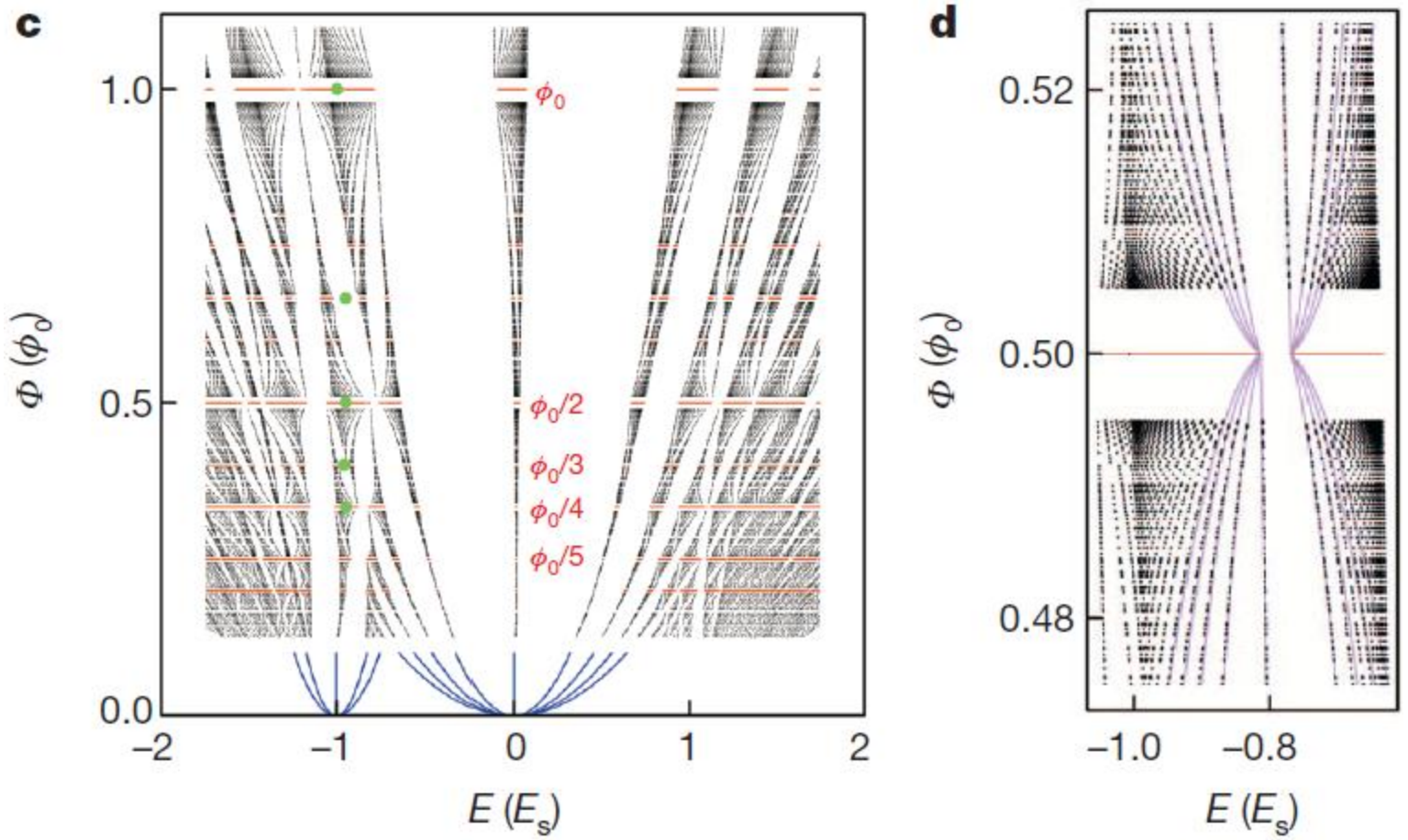

L.A. Ponomarenko et al., Nature **497**, 594 (2013)

BLG/hBN

BLG

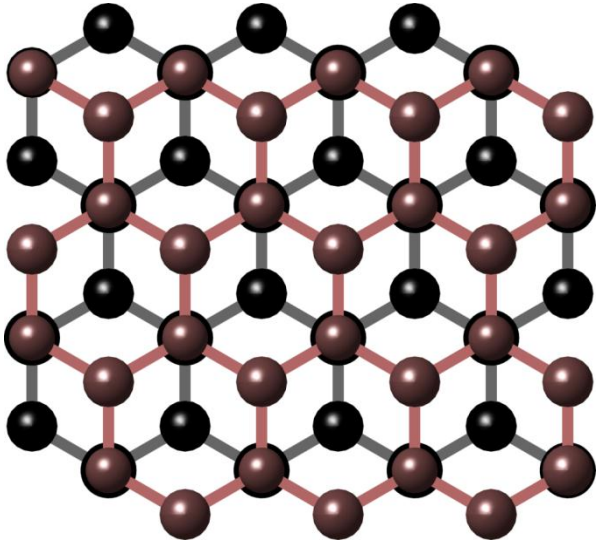

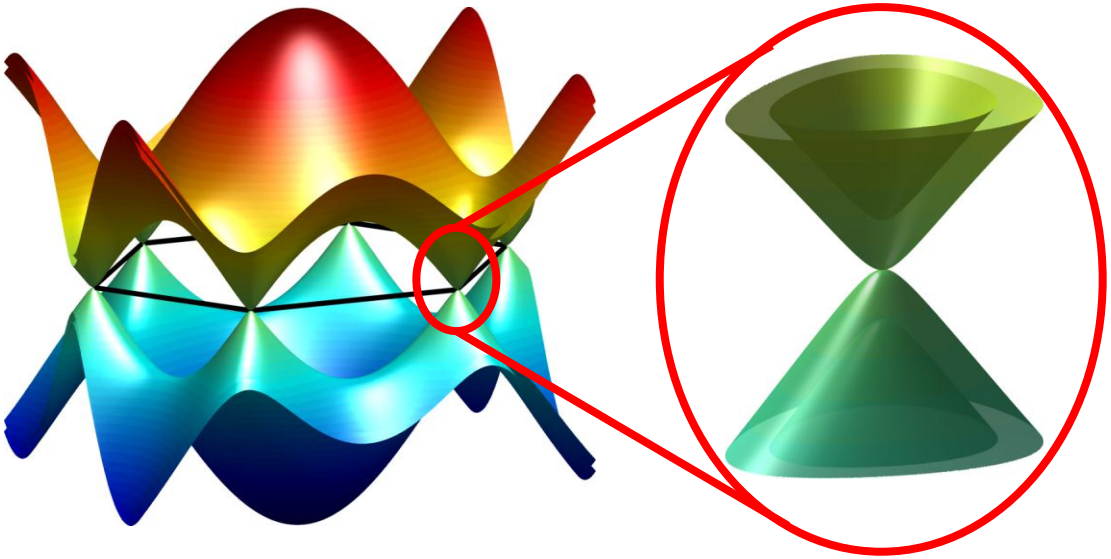

BLG/hBN

$$\hat{H} = \begin{pmatrix} v_3(\boldsymbol{\sigma}\cdot p)^T & v\boldsymbol{\sigma}\cdot p \\ v\boldsymbol{\sigma}\cdot p & \gamma_1\sigma_x\tau_z \end{pmatrix} +$$

$$\frac{1}{2}vb\left[\begin{pmatrix} g_+(r)(1+\sigma_z\tau_z) & 0 \\ 0 & g_-(r)(1-\sigma_z\tau_z) \end{pmatrix} - \begin{pmatrix} 0 & g^*(r)(\tau_z\sigma_x+i\sigma_y) \\ g(r)(\tau_z\sigma_x-i\sigma_y) & 0 \end{pmatrix}\right]$$

$$g_\pm(\boldsymbol{r}) = u_0\sum_n e^{i\boldsymbol{b_n}\cdot\boldsymbol{r}} \pm iu_3\sum_n(-1)^n e^{i\boldsymbol{b_n}\cdot\boldsymbol{r}}, \quad g(\boldsymbol{r}) = (u_2+iu_1\tau_z)\sum_n(-1)^n e^{i\boldsymbol{b_n}\cdot\boldsymbol{r}}(\hat{b}_n^x + i\hat{b}_n^y\tau_z)$$

BLG/hBN

$$\hat{H} = \begin{pmatrix} v_3(\sigma\cdot p)^T & v\sigma\cdot p \\ v\sigma\cdot p & \gamma_1\sigma_x\tau_z \end{pmatrix} +$$

$$\frac{1}{2}vb\left[\begin{pmatrix} g_+(r)(1+\sigma_z\tau_z) & 0 \\ 0 & g_-(r)(1-\sigma_z\tau_z) \end{pmatrix} - \begin{pmatrix} 0 & g^*(r)(\tau_z\sigma_x+i\sigma_y) \\ g(r)(\tau_z\sigma_x-i\sigma_y) & 0 \end{pmatrix}\right]$$

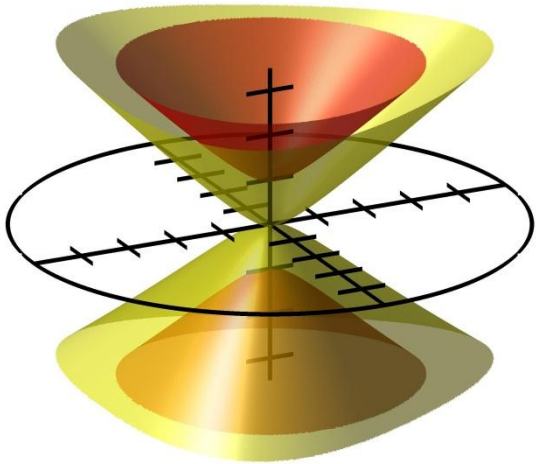

1. Interlayer symmetry breaking
2. Interplay between two energy scales: moiré and inter-layer coupling
3. Different chirality of carriers
4. Spectrum is no longer radially symmetric

BLG/hBN

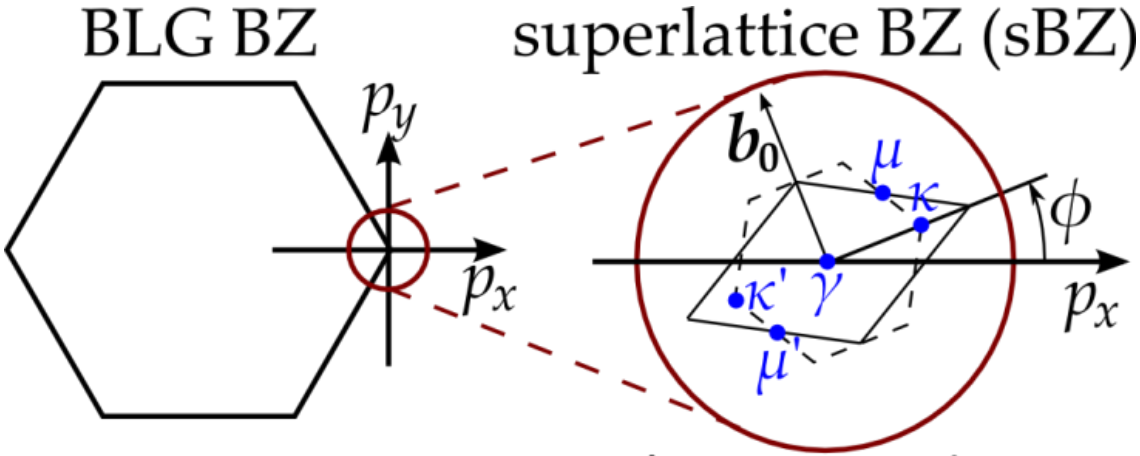

$$b_n = \hat{R}_{n\pi/3}[1-(1+\delta)^{-1}\hat{R}_{\theta}](0,\tfrac{4\pi}{\sqrt{3}a})$$

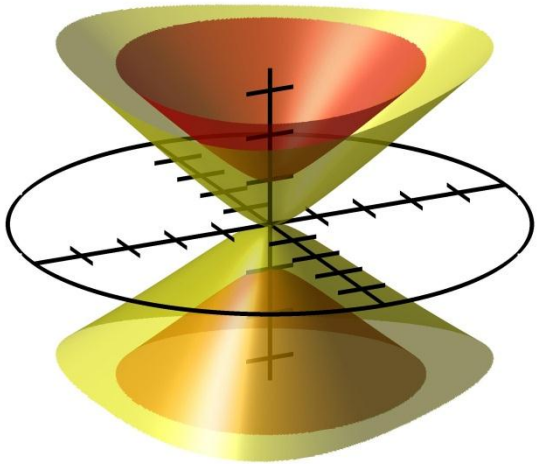

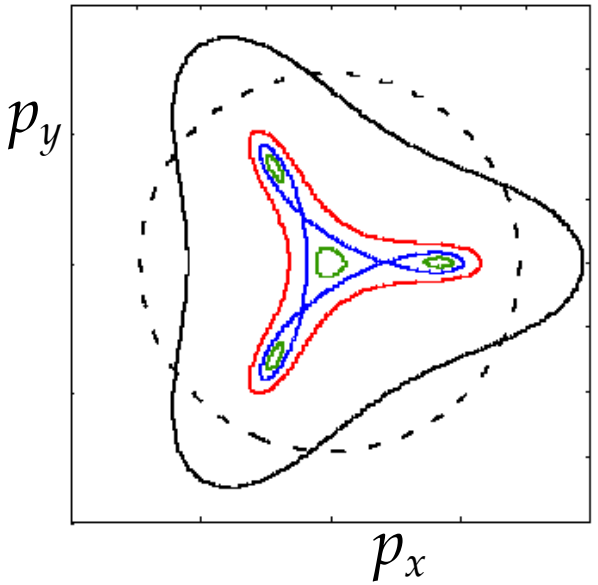

$(\theta = 0)$

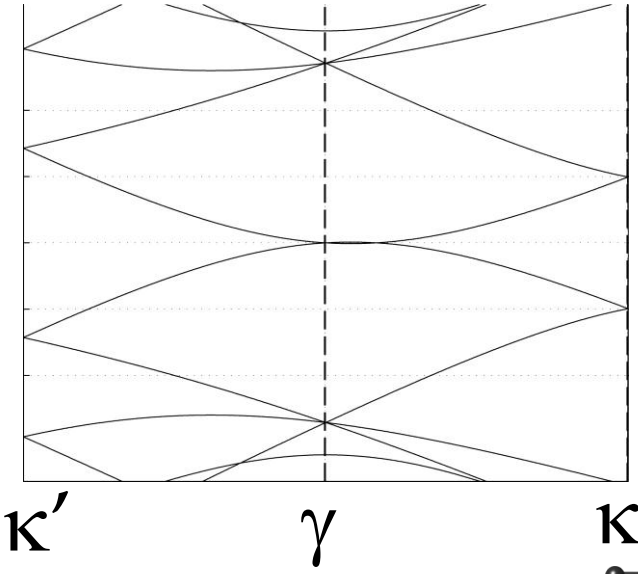

Valence band

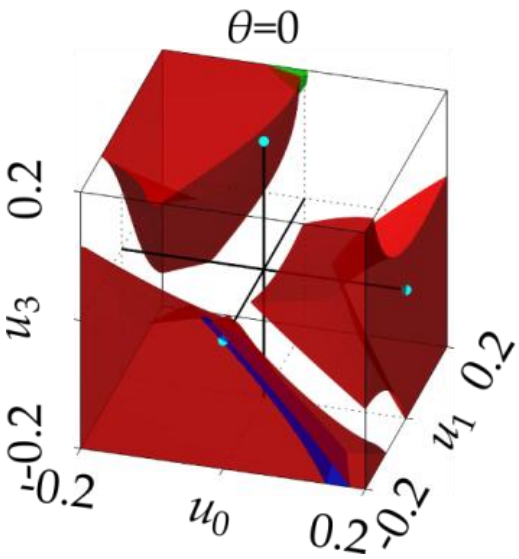

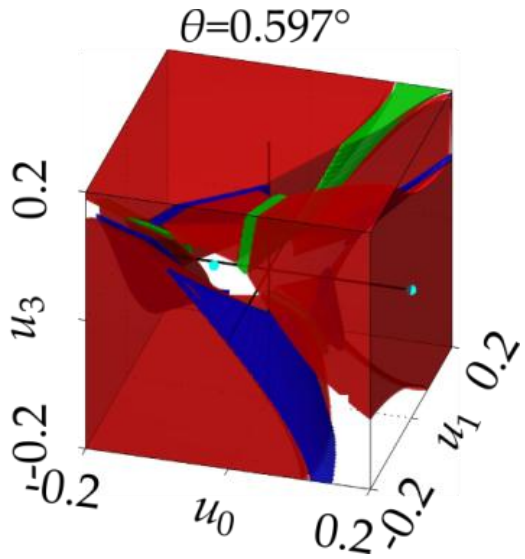

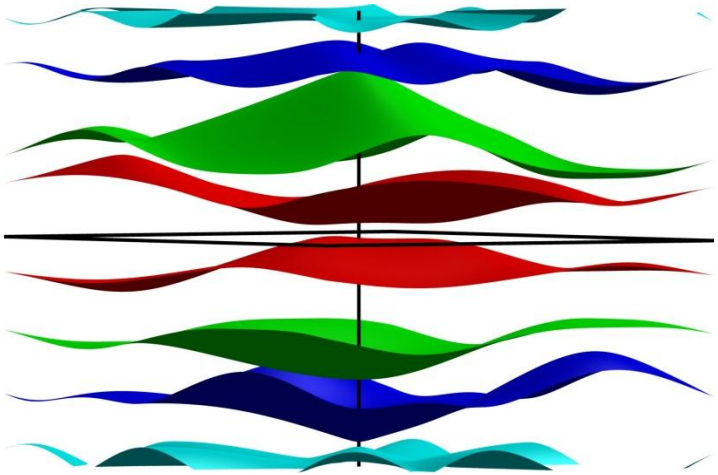

Gap at zero energy due to layer symmetry breaking

$$\Delta \approx 12u_3(u_1\cos\phi + u_2\sin\phi) + 6u_0^2(u_0 + u_3)$$

BLG/hBN

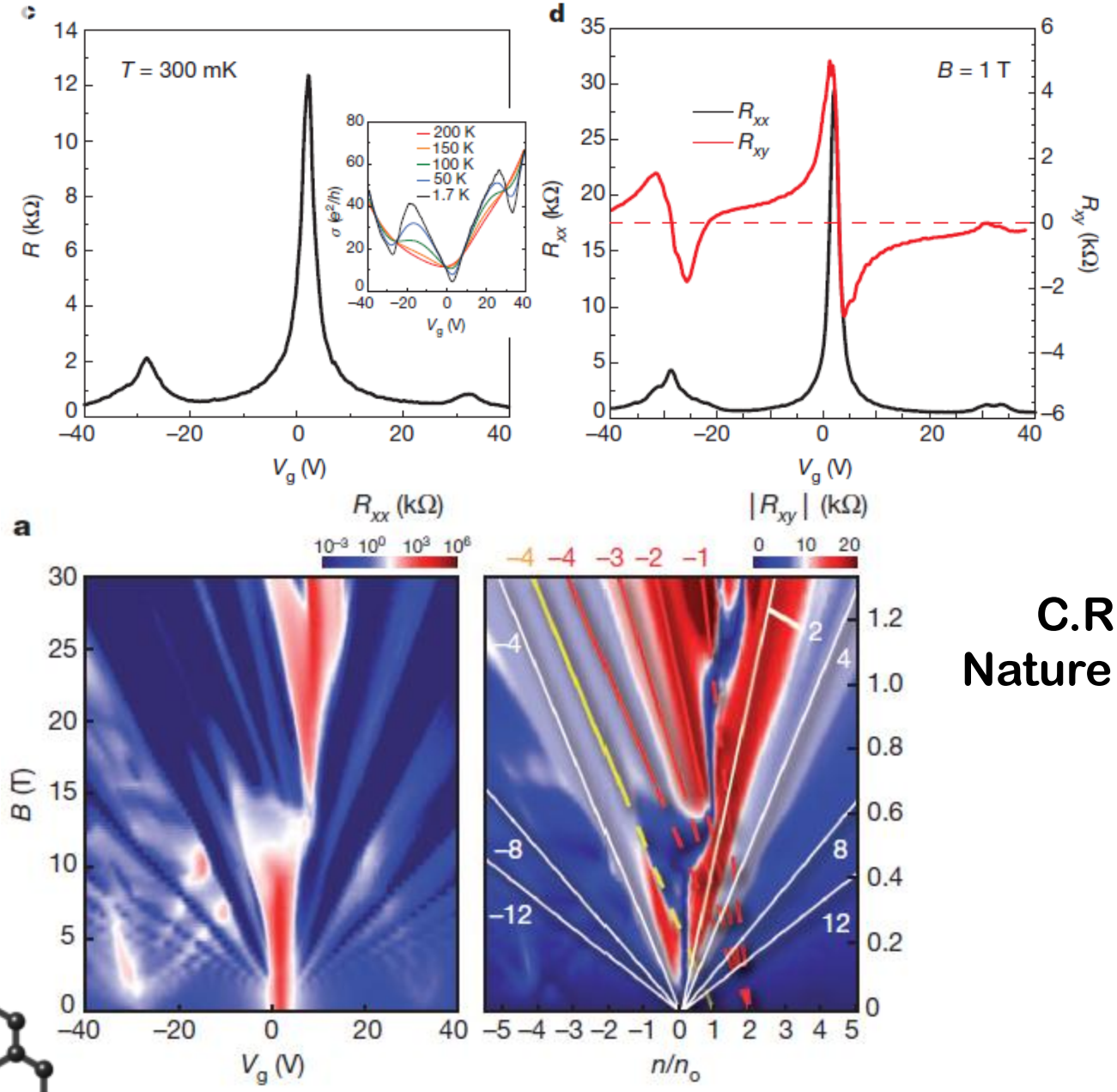

C.R. Dean et al.,
Nature **497**, 598 (2013)

Summary

- Bragg scattering of graphene electrons on the moiré potential leads to formation of minibands
- Monolayer graphene:
  - Periodic inversion-symmetric potential preserves the Dirac point
  - Secondary Dirac points created at the edges of the first miniband on the conduction/valence band (may be obscured by other spectral features)
- Bilayer graphene:
  - Even inversion-symmetric potential opens a gap at the neutrality point because the moiré potential breaks interlayer symmetry
  - Formation of gaps between the first and other minibands probable
  - Interplay between the misalignment angle θ and trigonal warping of the band structure